Polybis(1-methyl-2-thioimidazolate)iron(II): Crystal Structure and Magnetic Properties of a One-Dimensional Material Exhibiting Ferromagnetic Ordering below 8 K

Steven J. Rettig, Victor Sánchez, Alan Storr,* Robert C. Thompson,* and James Trotter

Department of Chemistry, University of British Columbia, Vancouver, British Columbia, Canada V6T 1Z1

Received June 30, 1999

Introduction

Diazolate ligands are well-known to bridge transition metal ions and to mediate magnetic interactions between paramagnetic centers.[1−3] The ability of 1,2-diazolates to form double bridges between transition metal ions and 1-D extended chain structures in which the metal ions are antiferromagnetically coupled via the ligands has been well documented in our reports on binary M(II) pyrazolates (M = Mn, Co, Ni, or Cu).[4−8] In contrast, metal polymers formed with bridging imidazolate ligands are of higher dimensionality (2-D or 3-D) as a result of the 1,3-positioning of the N-donor atoms of the imidazolate moiety, which allows only the formation of single bridges between metal centers.[9−14] Recently we have reported two extended 3-D lattices involving Fe(II) centers singly bridged by imidazolate ligands.[15,16] In both cases, magnetic studies revealed a critical temperature above which there is antiferromagnetic coupling between the paramagnetic centers and below which long-range ferromagnetic ordering occurs.

As a continuation of our studies on how structure and magnetism in metal diazolate compounds are correlated, we have examined the product formed by the reaction of the substituted imidazole 1-methyl-2-thiolimidazole with ferrocene. It was anticipated that with the N-1 position blocked with a methyl substituent, deprotonation of the thiol functionality would generate a bridging ligand, 1-Me-2-S-imid, capable of forming double bridges between Fe(II) centers in a rodlike polymer. Previous studies had revealed this type of bonding mode for this ligand in the dimeric molecules $[Me_2Ga(1\text{-Me-2-S-imid})]_2$ and $[Mo(\eta^3\text{-}C_3H_5)(CO)_2(1\text{-Me-2-S-imid})]_2$.[17] The rodlike 1-D structural motif was observed in the material characterized here, $[Fe(1\text{-Me-2-S-imid})_2\cdot 0.5Cp_2Fe]_x$. Interestingly, the phenomenon of long-range ferromagnetic ordering below a critical temperature, previously seen only in diazolate complexes with 2-D or 3-D extended lattices,[15,16,18] is observed here.

Experimental Section

Synthesis. $[Fe(1\text{-Me-2-S-imid})_2\cdot 0.5Cp_2Fe]_x$ was obtained by combining ferrocene (0.5 g, 2.68 mmol) and an excess of 1-methyl-2-thiolimidazole (1.5 g, 13.14 mmol) in a Carius tube sealed under vacuum. This mixture was heated at 145 °C for 6 days. During this period, a dark red solution of ferrocene in the molten imidazole was obtained, and light yellow crystals were deposited from the solution. The reaction mixture was then allowed to cool to room temperature, and the Carius tube was opened under a dinitrogen atmosphere. The excess of ligand was extracted with dry and oxygen-free acetonitrile, and residual ferrocene was removed with dry toluene. The compound was isolated as crystalline golden needles. Anal. Calcd for $C_{13}H_{15}Fe_{1.5}N_4S_2$: C, 41.6; H, 4.0; N, 14.9. Found; C, 41.5; H, 4.0; N, 14.7.

Physical Measurements. Magnetic susceptibilities were measured utilizing a Quantum Design (MPMS) SQUID magnetometer. The sample holder and details regarding the use of the equipment have been described elsewhere.[6a] Magnetic susceptibilities were corrected for the background signal of the sample holder and for diamagnetic susceptibilities of all atoms (-200×10^{-6} cm^3 mol^{-1}). Measurements were made from 2 to 300 K at three different fields: 500, 10 000, and 50 000 G. Magnetization versus applied field measurements were made at fields ranging from 0 to 55 000 G at temperatures of 2, 4.8, and 15 K. Hysteresis magnetization data were obtained by oscillating the applied magnetic field between +55 000 and −55 000 G at 4.8 K. All magnetic measurements were done on macroscopic crystals ground to a fine powder.

Thermal gravimetric analysis (35−800 °C) was done using a TA Instruments TA 2000 system with a TGA 51 unit.

X-ray Crystallographic Analysis. Crystallographic data for $[Fe(1\text{-Me-2-S-imid})_2\cdot 0.5Cp_2Fe]_x$ are shown in Table 1. A golden needle crystal having approximate dimensions of 0.04 × 0.08 × 0.45 mm was mounted on a Rigaku/ADSC CCD diffractometer and used for data collection. Diffraction data were collected at 180 K. Final unit cell parameters were obtained by least-squares fitting on the setting angles for 8103 reflections with $2\theta = 4.0-60.0°$. The data were processed[19] and corrected for Lorentz and polarization effects. The structure was solved by direct methods[20] and expanded using Fourier techniques.[21] The Fe atoms in the polymer chain lie at points of S_4 symmetry. The ferrocene Fe atom lies on a 4-fold axis; consequently, the Cp rings are massively disordered. Numerous models for Cp rings were tried, but the best model in terms of accounting for the electron density in the region was obtained by simple refinement of the two

* Authors to whom enquiries may be addressed. Telephone: R. C. Thompson, (604) 822-4979; A. Storr, (604) 822-3962. Fax: (604) 822-2847. E-mail: thompson@chem.ubc.ca; storr@chem.ubc.ca.

(1) La-Monica, G.; Ardizzoia, G. A. *Prog. Inorg. Chem.* **1997**, *46*, 151.
(2) Steel, P. J. *Coord. Chem. Rev.* **1990**, *106*, 227.
(3) (a) Trofimenko, S. *Prog. Inorg. Chem.* **1986**, *34*, 115. (b) Trofimenko, S. *Chem. Rev.* **1972**, *72*, 497.
(4) Ehlert, M. K.; Storr, A.; Thompson, R. C. *Can. J. Chem.* (a) **1992**, *70*, 1121; (b) **1993**, *71*, 1412.
(5) Ehlert, M. K.; Rettig, S. J.; Storr, A.; Thompson, R. C.; Einstein, F. W. B.; Batchelor, R. J. *Can. J. Chem.* **1993**, *71*, 331.
(6) Ehlert, M. K.; Rettig, S. J.; Storr, A.; Thompson, R. C.; Trotter, J. *Can. J. Chem.* (a) **1989**, *67*, 1970; (b) **1990**, *68*, 1444; (c) **1990**, *68*, 1494; (d) **1991**, *69*, 432; (e) **1992**, *70*, 2161; (f) **1993**, *71*, 1425.
(7) Ehlert, M. K.; Storr, A.; Summers, D. A.; Thompson, R. C. *Can. J. Chem.* **1997**, *75*, 491.
(8) Storr, A.; Summers, D. A.; Thompson, R. C. *Can. J. Chem.* **1998**, *76*, 1130.
(9) Jarvis, J. A. J.; Wells, A. F. *Acta Crystallogr.* **1960**, *13*, 1027.
(10) Freeman, H. C. *Adv. Protein Chem.* **1967**, *22*, 257.
(11) Strum, M.; Brandl, F.; Engel, D.; Hoppe, W. *Acta Crystallogr.* **1975**, *B31*, 2369.
(12) Lundberg, B. K. S. *Acta Chem. Scand.* **1972**, *26*, 3902.
(13) Cohen, I. A.; Ostfeld, D. *ACS Symp. Ser.* **1974**, *No. 5*, 221.
(14) Chaudhuri, P.; Karpenstein, I.; Winter, M.; Butzlaff, C.; Bill, E.; Trautwein, A. X.; Florke, U.; Haupt, H.-J. *J. Chem. Soc., Chem. Commun.* **1992**, 321.
(15) Rettig, S. J.; Storr, A.; Summers, D. A.; Thompson, R. C.; Trotter, J. *J. Am. Chem. Soc.* **1997**, *119*, 8675.
(16) Rettig, S. J.; Storr, A.; Summers, D. A.; Thompson, R. C.; Trotter, J. *Can. J. Chem.* **1999**, *77*, 425.
(17) Cooper, D. A.; Rettig, S. J.; Storr, A.; Trotter, J. *Can. J. Chem.* **1986**, *64*, 1643.
(18) Martinez-Lorente, M. A.; Petrouleas, V.; Poinsot, R.; Tuchagues, J. P.; Savariault, J. M.; Drillon, M. *Inorg. Chem.* **1991**, *30*, 3587.
(19) *teXsan: Crystal Structure Analysis Package*; Molecular Structure Corporation: 1985 and 1992.
(20) Gilmore, C. J. *MITHRIL90*; MITHRIL-an integrated direct methods computer program; University of Glasgow: Scotland, 1990.
(21) Beurskens, P. T.; Admiral, G.; Beurskens, G.; Bosman, W. P.; de Gelder, R.; Israel, R.; Smits, J. M. M. *DIRDIF94*: The DIRDIF-94 program system; Technical Report of the Crystallography Laboratory; University of Nijmegen: The Netherlands, 1994.

10.1021/ic990774k CCC: $18.00
Published on Web 11/20/1999

Table 1. Crystallographic Data for $[Fe(1\text{-Me-2-S-imid})_2 \cdot 0.5Cp_2Fe]_x$[a]

formula	$C_{13}H_{15}Fe_{1.5}N_4S_2$
fw	375.18
space group	*P*4/*n* (No. 85)
a, Å	13.2862(7)
c, Å	8.7665(4)
V, Å^3	1547.49(11)
Z	4
ρ_{calc}, g/cm^3	1.610
F(000)	768
radiation	Mo
μ, cm^{-1}	16.88
λ, Å	0.71069
R	0.077
R_w	0.063
T, °C	−93

[a] $R = \sum||F_o^2| - |F_c^2||/\sum|F_o^2|$, $R_w = (\sum w(|F_o^2| - |F_c^2|)^2/\sum wF_o^4)^{1/2}$.

Table 2. Selected Bond Lengths (Å) and Angles (deg) for $[Fe(1\text{-Me-2-S-imid})_2 \cdot 0.5Cp_2Fe]_x$[a]

Fe(1)−S(1)	2.3677(8)	Fe(2)−N(1)	2.054(2)
S(1)−C(1)	1.732(3)	N(1)−C(1)	1.342(3)
N(1)−C(2)	1.383(4)	N(2)−C(1)	1.364(3)
N(2)−C(3)	1.375(4)	N(2)−C(4)	1.455(4)
C(2)−C(3)	1.358(4)		
S(1)−Fe(1)−S(1)[a]	110.05(2)	S(1)−Fe(1)−S(1)[b]	110.05(2)
S(1)−Fe(1)−S(1)[c]	108.32(4)	N(1)−Fe(2)−N(1)[d]	104.91(6)
N(1)−Fe(2)−N(1)[e]	104.91(6)	N(1)−Fe(2)−N(1)[c]	119.05(13)
Fe(1)−S(1)−C(1)	95.67(10)	Fe(2)−N(1)−C(1)	125.9(2)
Fe(2)−N(1)−C(2)	128.0(2)	C(1)−N(1)−C(2)	106.0(2)
C(1)−N(2)−C(3)	108.0(3)	C(1)−N(2)−C(4)	126.5(3)
C(3)−N(2)−C(4)	125.5(3)	S(1)−C(1)−N(1)	125.4(2)
S(1)−C(1)−N(2)	124.7(2)	N(1)−C(1)−N(2)	109.9(3)
N(1)−C(2)−C(3)	109.9(3)	N(2)−C(3)−C(2)	106.2(3)

[a] Superscript letters refer to symmetry operation. (a) $^1/_2 + y$, $1 - x$, $-z$. (b) $1 - y$, $-^1/_2 + x$, $-z$. (c) $^3/_2 - x$, $^1/_2 - y$, z. (d) $^1/_2 + y$,$1 - x$,$1 - z$. (e) $1 - y$, $-^1/_2 + x$, $1 - z$.

large and two smaller peaks in the region. The site occupancy factors for each Cp ring were adjusted to give a total of 1.25 C atoms and approximately equal thermal parameters. For each Cp ring, the major and minor peaks were assigned populations of 0.9 and 0.35, respectively. The geometry of the ferrocene is poorly determined due to the disorder and is omitted from the tables. The two 0.35 occupancy Cp carbon atoms, C(6) and C(8), were refined isotropically, and the remaining non-hydrogen atoms were refined anisotropically. The Cp H atoms were omitted from the model, and the remaining hydrogen atoms were fixed in calculated positions with C−H = 0.98 Å. Selected bond lengths and bond angles are shown in Table 2. Final atomic coordinates and equivalent isotropic thermal parameters, hydrogen atom parameters, anisotropic thermal parameters, torsion angles, and nonbonded contacts are included as supporting information.

Results and Discussion

The structure of a section of the polymer chain is shown in Figure 1, and a view of the lattice perpendicular to the polymer chains is depicted in Figure 2. The structure consists of chains of distorted tetrahedral iron(II) ions double bridged by the 1-methyl-2-thioimidazolate ligands, giving rise to eight-membered rings linked by the Fe ions in a pseudospiro conformation (Figure 1). The ligands bind through the unsubstituted nitrogen (N(1) in Figure 1) and the sulfur atoms and orient along the chain in a manner that leads to distinctive FeN_4 and FeS_4 chromophores which alternate throughout the polymer chains. These structural characteristics produce a rodlike shape to the polymeric chain. The Fe(2)−N bond distances are significantly shorter at 2.054 Å than the Fe(1)−S bonds at 2.368 Å. The S−Fe(1)−S bond angles are close to tetrahedral, ranging from 108.32° to 110.05°, while the N−Fe(2)−N angles are

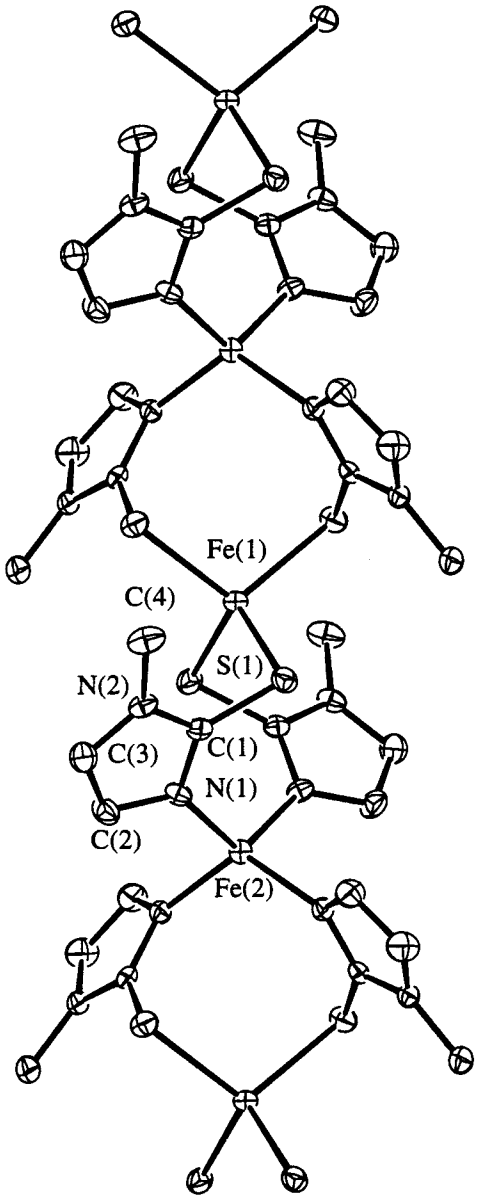

Figure 1. Molecular structure of a section of the polymer chain showing the atom numbering scheme; 33% probability thermal ellipsoids are shown.

further from tetrahedral, ranging from 104.91° to 119.05°. Molecules of ferrocene, one for every two repeating units in the chain, are trapped between the polymer chains (Figure 2). These molecules cannot be removed by thermolysis without decomposition of the polymer. Thermal gravimetric analysis (TGA) shows the material to be thermally stable to 197 °C. Decomposition with continuous weight loss occurs from 197 to 800 °C with a total weight loss of 69% of the initial mass. This compares favorably to a 65% loss that would occur if FeS remains.

Magnetic susceptibility and χT versus temperature data on powdered samples of $[Fe(1\text{-Me-2-S-imid})_2 \cdot 0.5Cp_2Fe]_x$ in an applied magnetic field of 500 G are shown in Figure 3. As the temperature is lowered from 300 K, the χT value decreases. At about 8 K, χT increases abruptly, reaching a maximum at about 5 K before decreasing with decreasing temperature in the lowest temperature region. The behavior suggests antiferromagnetic exchange between metal centers above the critical temperature, T_c, of 8 K and a ferromagnetic transition below this temperature. Support for a ferromagnetic transition comes from magnetization

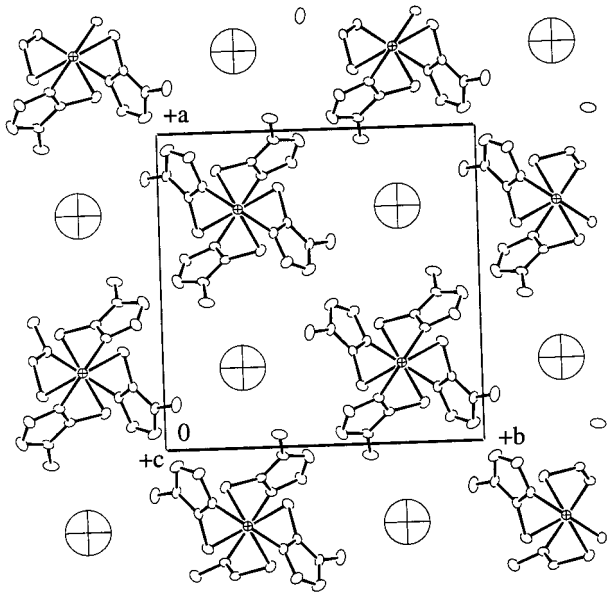

Figure 2. View of the crystal structure down the *c* axis. Crossed-circles represent molecules of ferrocene; 33% thermal ellipsoids are shown.

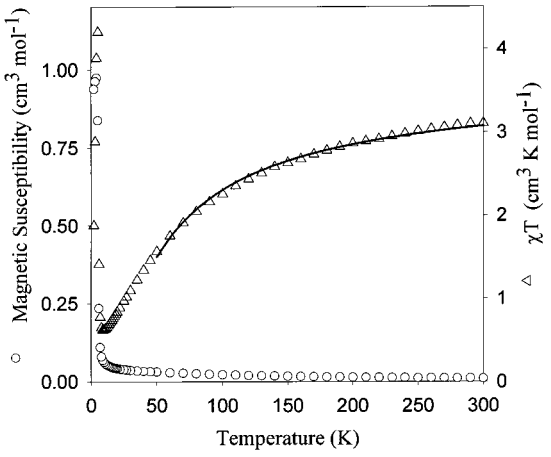

Figure 3. Magnetic susceptibility and χT versus temperature at 500 G. The line is from theory as described in the text.

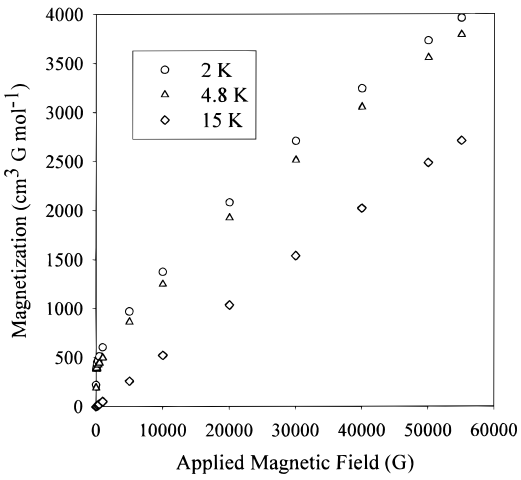

Figure 4. Plot of magnetization versus applied field at three temperatures.

versus applied field plots at different temperatures (Figure 4). At 15 K (above T_c), the plot is linear to over 20 000 G and extrapolates to zero magnetization at zero applied field. At temperatures below T_c, the plots are not linear and extrapolate

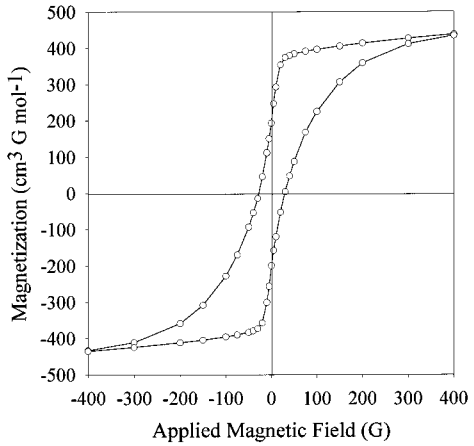

Figure 5. Field dependence of magnetization at 4.8 K. Central portion of hysteresis loop shown.

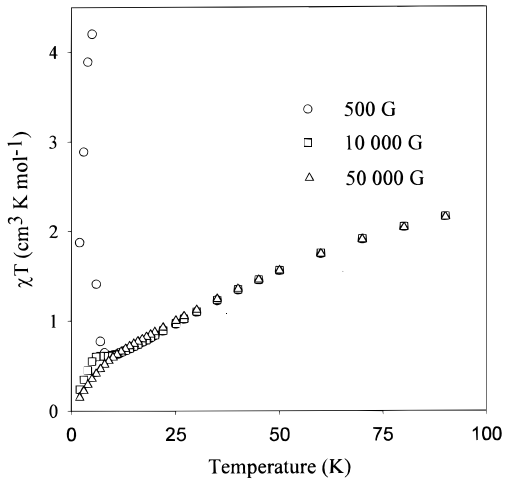

Figure 6. Plot of χT versus temperature at three values of applied field.

to yield net magnetization at zero applied field. Cycling the applied field between +55 000 and −55 000 G at 4.8 K generates a hysteresis loop (Figure 5), as expected for a material exhibiting long-range ferromagnetic ordering. From this hysteresis loop, a coersive field of 40 G and a remnant magnetization of 190 cm^3 G mol^{-1} are obtained. We measured magnetic susceptibilities as a function of temperature at 10 000 and 50 000 G as well as at 500 G (Figure 6). The results show field dependence at low temperatures, particularly below T_c. The magnetic transition which is clearly seen in the 500 G data is much less pronounced in the 10 000 G data and is absent at 50 000 G. The ferromagnetic ordering is clearly repressed by applied fields.

The magnetic properties of $[Fe(1\text{-Me-}2\text{-S-imid})_2 \cdot 0.5Cp_2Fe]_x$ parallel closely those of $[Fe_3(imid)_6(imidH)_2]_x$,[15] $[Fe(4\text{-imidazol-acetate})_2]_x$,[18] and $[Fe(2\text{-Me-imid})_2 \cdot 0.13Cp_2Fe]_x$,[16] compounds for which the primary exchange process is considered to involve antiferromagnetic coupling between iron centers with a canting of the spins. A spin-canted structure for the compound studied here is also supported by the fact that the highest magnetization reached (3960 cm^3 G mol^{-1} at 2 K and 55 000 G) is significantly smaller than the theoretical saturation value (22 300 cm^3 G mol^{-1}).[22] Additional support for a canted spin structure comes from structural data which show a feature characteristic of such systems, that of a systematic alternation of the relative orienta-

(22) Carlin, R. L. *Magnetochemistry*; Springer-Verlag: Berlin, 1986.

tion of neighboring metal chromophores.[15] As a measure of this, the dihedral angle between the S(1)−Fe(1)−S(1)^c and N(1)^d−Fe(2)−N(1)^e planes is 27.6°. We conclude that antiferromagnetic coupling between neighboring metal centers along the chain occurs with imperfect antiparallel alignment of spins, leading to residual spin on the chains. Ferromagnetic ordering of the residual spins generates long-range three-dimensional magnetic ordering and spontaneous magnetization at low temperatures. It should be noted that the chains in $[Fe(1\text{-Me-2-S-imid})_2 \cdot 0.5Cp_2Fe]_x$ are isolated (Figure 2), and therefore, any interchain interaction cannot be mediated by bonding interactions. This contrasts with the situation for $[Fe_3(imid)_6(imid\text{-}H)_2]_x$[15] and $[Fe(2\text{-Me-imid})_2 \cdot 0.13Cp_2Fe]_x$[16] where covalent bonding interactions connect the paramagnetic centers in three dimensions and for $[Fe(4\text{-imidazolacetate})_2]_x$[18] where hydrogen-bonding interactions connect sheets of covalently linked metal centers. Such considerations may play an important role in determining the magnitude of the coersive field in these systems, as $[Fe(1\text{-Me-2-S-imid})_2 \cdot 0.5Cp_2Fe]_x$ exhibits the smallest coersive field of the four compounds considered here.

To obtain further evidence in support of the intrachain coupling in $[Fe(1\text{-Me-2-S-imid})_2 \cdot 0.5Cp_2Fe]_x$, we examined fits of the magnetic susceptibility to the expression derived employing an isotropic Hamiltonian of the form $H = -2JS_1 \cdot S_2$ for a linear chain of antiferromagnetically coupled $S = 2$ centers.[23] The equation is

$$\chi = (Ng^2\beta^2/kT)\left[\frac{2 + 71.938x^2}{1 + 10.482x + 955.56x^3}\right]$$

where $x = |J|/kT$, J is the exchange coupling constant, and g is the Landé factor. By employing susceptibility data obtained at the three different fields (500, 10 000, and 50 000 G), we were unable to obtain satisfactory fits when data below 50 K were included. Good fits were, however, obtained for data in the range 50−300 K as is illustrated for the 500 G χT data in Figure 3. The lack of agreement between theory and experiment at low temperatures is not surprising since the model does not accommodate the effects of residual spin due to spin canting or interchain interactions, both of which are more pronounced at low temperatures. The theory line shown in Figure 3 was calculated with $-J = 3.92$ cm^{-1} and $g = 2.21$ ($F = 0.000\,33$). In the fitting procedure, the function F, which provides a measure of the goodness of fit, was minimized:

$$F = \left[\frac{1}{n}\sum_{i=1}^{n}\left[\frac{\chi^i_{calc} - \chi^i_{obs}}{\chi^i_{obs}}\right]^2\right]^{1/2}$$

where n is the number of data points. The model used is limited by the fact it employs a single g value, while the structure of the compound requires different g values for the FeN_4 and FeS_4 chromophores. The best-fit g value of 2.21 presumably approximates the average g for the system. The strength of the antiferromagnetic coupling in this compound, as judged by the magnitude of $-J$, seems to be slightly greater than that seen in $[Fe_3(imid)_6(imid\text{-}H)_2]_x$[15] and $[Fe(2\text{-Me-imid})_2 \cdot 0.13Cp_2Fe]_x$[16] for which $-J$ values of 2.3 and 2.75, respectively, have been reported.

The alternation in chromophore type and, therefore, g value along the chain should generate important magnetic consequences for this antiferromagnetically coupled system. The size of the individual magnetic dipoles will alternate along the chain, and even perfect antiparallel alignment between neighbors would lead to a residual moment on the chain—an example of ferrimagnetism. While this may contribute to the observed magnetic properties of this system, a simple calculation indicates it cannot be the sole source of the residual chain magnetization. The saturation magnetization, M_{sat}, for an $S = 2$ center is[22]

$$M_{sat} = Ng\beta S$$

The net saturation magnetization, M_{net}, for a chain of perfect antiparallel coupled $S = 2$ metal centers with regularly alternating g values is, per mole of metal center,

$$M_{net} = {}^1/_2\Delta M_{sat} = N\beta\Delta g$$

Inserting 3960 cm^3 G mol^{-1} (the magnetization measured at 2 K and 55 000 G) for M_{net} in the above equation yields a Δg of 0.71. Hence, an unrealistically large difference in g values for the FeN_4 and FeS_4 chromophores would be required to invoke ferrimagnetism to account for the largest magnetization (not even saturation magnetization) observed. We conclude that spin canting is the primary source of the residual magnetization on the chains, although we cannot rule out ferrimagnetism as a contributing factor.

Acknowledgment. We thank the Natural Sciences and Engineering Research Council of Canada for financial support and P. Borda of this department for C, H, N analyses.

Supporting Information Available: Tables of crystallographic data, atomic coordinates, bond lengths, bond angles, anisotropic thermal parameters for non-H atoms, bond lengths and angles involving hydrogen, torsion angles, and nonbonded contacts for the compound. This material is available free of charge via the Internet at http://pubs.acs.org.

IC990774K

(23) Hiller, W.; Strahle, J.; Datz, A.; Hanack, M.; Hatfield, W. F.; Gutlich, P. *J. Am. Chem. Soc.* **1984**, *106*, 329.